Spectrum and vibrational predissociation of the HF dimer. I. Bound and quasibound states

G. W. M. Vissers, G. C. Groenenboom, and A. van der Avoird[a)]
Institute of Theoretical Chemistry, NSRIM Center, University of Nijmegen, Toernooiveld, 6525 ED Nijmegen, The Netherlands

(Received 30 December 2002; accepted 2 April 2003)

We present full six-dimensional calculations of the bound states of the HF dimer for total angular momentum $J=0,1$ and of the quasibound states for $J=0$ that correspond with vibrational excitation of one of the HF monomers, either the donor or the acceptor in the hydrogen bond. Transition frequencies and rotational constants were calculated for all four molecular symmetry blocks. A contracted discrete variable representation basis was used for the dimer and monomer stretch coordinates R, r_A, r_B; the generation of the monomer basis in the dimer potential leads to significantly better convergence of the energies. We employed two different potential energy surfaces: the SQSBDE potential of Quack and Suhm and the SO-3 potential of Klopper, Quack, and Suhm. The frequencies calculated with the SO-3 potential agree very well with experimental data and are significantly better than those from the SQSBDE potential. © *2003 American Institute of Physics.* [DOI: 10.1063/1.1577111]

I. INTRODUCTION

One of the most important interactions in nature is the hydrogen bond. Quantitative information about the dynamics of hydrogen-bonded systems can be obtained by the study of small model systems, such as $(HF)_2$, $(HCl)_2$,[1–3] and $(H_2O)_2$.[4–8] The present paper focuses on the HF dimer, which has been widely studied. On the experimental side, much work has been done to determine its structure and tunneling dynamics,[9–14] vibrational predissociation lifetimes,[15–20] and rotational product state distributions.[21–24] On the theoretical side, the dimer has also been studied in a variety of ways, using quantum Monte Carlo methods,[25–27] four-dimensional rigid rotor[28–31] and full six-dimensional (6D) bound state calculations,[32–37] as well as vibrational predissociation calculations.[33,37–39]

In the theoretical work, several potential energy surfaces (PESs) have been used,[25,40–42] of which the BJKKL surface[41] by Bunker *et al.* and the empirically adjusted SQSBDE surface[25] by Quack and Suhm have been the most popular. Recently, Klopper *et al.* published a new PES called SO-3,[43] which is based on explicitly correlated second-order Møller–Plesset calculations, and which is adjusted to reproduce the experimental dissociation energy and monomer stretch frequencies. This potential has been used to describe the dimer interactions in $He_n(HF)_2$ clusters[44] and the HF trimer,[45] but so far no rigorous test of this potential for the dimer proper has been published.

In this paper we present the results of full dimensional (6D) variational calculations on the SO-3 surface. We have computed bound states for $(HF)_2$ with both monomers in their vibrational ground state and total angular momentum $J=0,1$, as well as quasibound states where one of the monomers is vibrationally excited, for $J=0$. The same calculations have been performed on the SQSBDE surface, to allow for a fair comparison between the new potential and an older, high quality potential.

In the accompanying paper[46] (Paper II), we report results of 6D photodissociation calculations on vibrationally predissociating states of the SO-3 surface. We have calculated predissociation lifetimes and rotational state distributions upon excitation of the donor or the acceptor stretch, and combinations of these with excitations in the dimer stretch or the dimer geared bend modes. From the calculated rotational state distributions we have computed the theoretical photofragment angular state distributions, which allows us to compare with experimental data directly.

This paper is organized as follows: Section II will give the Hamiltonian for this system and the basis set used, Sec. III will deal with the details of the calculations. Results for both PESs will be presented and discussed in Sec. IV.

II. THEORY

The full-dimensional body fixed (BF) nuclear motion Hamiltonian for a dimer consisting of monomers A and B can be written as

$$\hat{H}=\hat{H}_0+V_I(R,\mathbf{r}_A,\mathbf{r}_B), \tag{1}$$

where V_I is the interaction potential between the two molecules. In the two-angle embedded frame of Fig. 1, the term $\hat{H}_0$ is given by

$$\hat{H}_0=\hat{h}_A+\hat{h}_B-\frac{\hbar^2}{2\mu}\frac{1}{R}\frac{\partial^2}{\partial R^2}R+\frac{\hat{J}^2+\hat{j}_{AB}^2-2\hat{\mathbf{j}}_{AB}\cdot\hat{\mathbf{J}}}{2\mu R^2}, \tag{2}$$

where μ is the reduced mass of the dimer, $\hat{\mathbf{J}}$ is the total angular momentum operator, and $\hat{\mathbf{j}}_{AB}$ is the vector sum of the monomer angular momentum operators $\hat{\mathbf{j}}_A$ and $\hat{\mathbf{j}}_B$. The monomer Hamiltonians $\hat{h}_X$, $X=A, B$ are given by

a)Electronic mail: avda@theochem.kun.nl

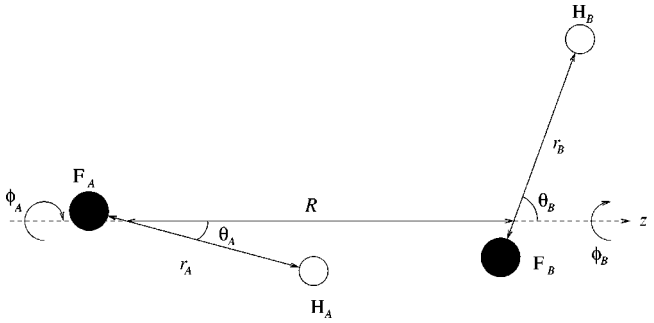

FIG. 1. Jacobi coordinates of the HF dimer. r_A and r_B denote the intramolecular distances and R is the distance between the two centers of mass. The vector $\mathbf{R}$ coincides with the z axis, and the angle between $\mathbf{R}$ and $\mathbf{r}_X$ is given by θ_X, for $X=A,B$. The torsional angle of monomer X is denoted by ϕ_X.

$$\hat{h}_X = -\frac{\hbar^2}{2\mu_X}\frac{1}{r_X}\frac{\partial^2}{\partial r_X^2} r_X + \frac{\hat{j}_X^2}{2\mu_X r_X^2} + V_X(r_X), \tag{3}$$

where μ_X denotes the reduced mass of monomer X, and V_X are the monomer potentials.

A matrix representation of the total Hamiltonian was calculated in a BF basis

$$|n v_A v_B (j_A j_B) j_{AB} K; JM\rangle = |n\rangle |v_A v_B\rangle |(j_A j_B) j_{AB} K; JM\rangle, \tag{4}$$

where $|n\rangle = \varphi_n(R)$ denotes a dimer stretch basis function, and $|v_A v_B\rangle = \chi_{v_A}(r_A)\chi_{v_B}(r_B)$ a product of monomer stretch functions. The angular basis functions are given by

$$|(j_A j_B) j_{AB} K; JM\rangle = \sqrt{\frac{(2j_A+1)(2j_B+1)(2J+1)}{64\pi^3}} D^{(J)}_{MK}(\alpha,\beta,0)^* \times \sum_{m_A m_B} C^{(j_A)}_{m_A}(\hat{\mathbf{r}}_A) C^{(j_B)}_{m_B}(\hat{\mathbf{r}}_B) \langle j_A m_A; j_B m_B | j_{AB} K\rangle, \tag{5}$$

where the $C^{(j_X)}_{m_X}(\hat{\mathbf{r}}_X)$ denote Racah-normalized spherical harmonical functions of the body fixed angles of monomer X, which are coupled with a Clebsch–Gordan coefficient $\langle j_A m_A; j_B m_B | j_{AB} K\rangle$. The Wigner rotation function $D^{(J)}_{MK}(\alpha,\beta,0)^*$ depends on the polar angles (α, β) of the intermolecular vector $\mathbf{R}$ with respect to a space fixed frame.

The dimer stretch functions are given by $\varphi_n(R) = \tilde{\varphi}_n(R)/R$, where the $\tilde{\varphi}_n(R)$ are eigenfunctions of a reference Hamiltonian,

$$\hat{h}^{\mathrm{ref}} = -\frac{\hbar^2}{2\mu}\frac{\partial^2}{\partial R^2} + V^{\mathrm{ref}}(R), \tag{6}$$

which will be specified further in the following. The eigenfunctions are obtained using a sinc-function discrete variable representation (DVR)[47] method. The monomer stretch basis functions $\chi_{v_X}(r_X) = \tilde{\chi}_{v_X}(r_X)/r_X$ are obtained in the same way.

Using these basis functions, the matrix elements of $\hat{H}_0$ are given by

$$\begin{aligned}
&\langle n' v_A' v_B' (j_A' j_B') j_{AB}' K'; JM | \hat{H}_0 | n v_A v_B (j_A j_B) j_{AB} K; JM\rangle \\
&= \delta_{j_A' j_A}\delta_{j_B' j_B}\delta_{j_{AB}' j_{AB}} \Big\{ \delta_{n'n}\delta_{v_A' v_A}\delta_{v_B' v_B}\delta_{K'K}(\epsilon_n + \epsilon_{v_A} + \epsilon_{v_B}) + \delta_{n'n}\delta_{K'K} \\
&\times \left[\frac{\hbar^2}{2\mu_A}\langle v_A' | r_A^{-2} | v_A\rangle j_A(j_A+1)\delta_{v_B' v_B} + \frac{\hbar^2}{2\mu_B}\langle v_B' | r_B^{-2} | v_B\rangle j_B(j_B+1)\delta_{v_A' v_A} \right] + \delta_{v_A' v_A}\delta_{v_B' v_B}\frac{\hbar^2}{2\mu}\langle n' | R^{-2} | n\rangle \\
&\times [\delta_{K'K}[J(J+1) + j_{AB}(j_{AB}+1) - 2K^2] - \delta_{K',K+1} C^+_{j_{AB}K} C^+_{JK} - \delta_{K',K-1} C^-_{j_{AB}K} C^-_{JK}] \Big\},
\end{aligned} \tag{7}$$

where ϵ_n is the nth eigenvalue of the dimer stretch reference Hamiltonian of Eq. (6), and ϵ_{v_A} and ϵ_{v_B} are the monomer stretch energies. The kinetic energy is diagonal in the angular basis, except for the Coriolis coupling terms $C^{\pm}_{IK} \equiv \sqrt{I(I+1) - K(K\pm 1)}$ that couple blocks with different K. However, this coupling is neglected, because it is absent for $J=0$, and generally small in the HF dimer for low values of J.[36]

The interaction potential V_I was expanded in angular functions of the type of Eq. (5). Since the potential is invari-

TABLE I. Projection operators $\hat{\mathcal{P}}^{\Gamma}$ for the irreps of PI(C_{2v}). $\hat{E}$ denotes the identity, $\hat{P}$ the exchange of the monomers, $\hat{E}^*$ spatial inversion, $\hat{P}^* = \hat{P}\hat{E}^* = \hat{E}^*\hat{P}$. The dimer stretch functions are invariant under all symmetry operations.

$\hat{P}\lvert v_A v_B (j_A j_B) j_{AB} K; JM\rangle$	=	$(-1)^{j_A+j_B+J} \lvert v_B v_A (j_B j_A) j_{AB} - K; JM\rangle$
$\hat{E}^* \lvert v_A v_B (j_A j_B) j_{AB} K; JM\rangle$	=	$(-1)^{j_A+j_B+j_{AB}+J} \lvert v_A v_B (j_A j_B) j_{AB} - K; JM\rangle$
$\hat{P}^* \lvert v_A v_B (j_A j_B) j_{AB} K; JM\rangle$	=	$(-1)^{j_{AB}} \lvert v_B v_A (j_B j_A) j_{AB} K; JM\rangle$
$\hat{\mathcal{P}}^{A_1} = \frac{1}{4}(\hat{E} + \hat{P} + \hat{E}^* + \hat{P}^*)$		$\hat{\mathcal{P}}^{B_1} = \frac{1}{4}(\hat{E} - \hat{P} - \hat{E}^* + \hat{P}^*)$
$\hat{\mathcal{P}}^{A_2} = \frac{1}{4}(\hat{E} + \hat{P} - \hat{E}^* - \hat{P}^*)$		$\hat{\mathcal{P}}^{B_2} = \frac{1}{4}(\hat{E} - \hat{P} + \hat{E}^* - \hat{P}^*)$

ant under overall rotations of the system, it does not depend on α and β, and not explicitly on both ϕ_A and ϕ_B, but only on the difference angle $\phi \equiv \phi_B - \phi_A$. Only the terms with $J=K=0$ appear in the expansion, so that the expansion functions can be written as

$$A_{L_A L_B L}(\theta_A,\theta_B,\phi) = (-1)^{L_A+L_B+L} \sum_{M_A} \begin{pmatrix} L_A & L_B & L \\ M_A & -M_A & 0 \end{pmatrix} \times C^{(L_A)}_{M_A}(\theta_A,0) C^{(L_B)}_{-M_A}(\theta_B,\phi). \quad (8)$$

The corresponding expansion coefficients $c_{L_A L_B L}(R,r_A,r_B)$ are then given by

$$c_{L_A L_B L}(R,r_A,r_B) = \frac{(2L_A+1)(2L_B+1)(2L+1)}{16\pi^2} \times \int d\cos\theta_A \int d\cos\theta_B \times \int d\phi\, A_{L_A L_B L}(\theta_A,\theta_B,\phi) \times V(R,r_A,r_B,\theta_A,\theta_B,\phi). \quad (9)$$

Substitution of this expansion for the potential results in the following expression for the potential matrix elements:

$$\begin{aligned} &\langle n' v'_A v'_B (j'_A j'_B) j'_{AB} K'; JM | V_I | n v_A v_B (j_A j_B) j_{AB} K; JM \rangle \\ &= \delta_{K'K} [(2j'_A+1)(2j_A+1)(2j'_B+1)(2j_B+1)(2j'_{AB}+1) \\ &\quad \times (2j_{AB}+1)]^{1/2} \sum_{L_A L_B L} \langle n' v'_A v'_B | c_{L_A L_B L} | n v_A v_B \rangle \\ &\quad \times (-1)^{j_A+j_B+j_{AB}+L_A+L_B-K} \begin{pmatrix} j'_A & L_A & j_A \\ 0 & 0 & 0 \end{pmatrix} \\ &\quad \times \begin{pmatrix} j'_B & L_B & j_B \\ 0 & 0 & 0 \end{pmatrix} \begin{pmatrix} j'_{AB} & L & j_{AB} \\ -K & 0 & K \end{pmatrix} \\ &\quad \times \begin{Bmatrix} j'_A & L_A & j_A \\ j'_B & L_B & j_B \\ j'_{AB} & L & j_{AB} \end{Bmatrix}. \end{aligned} \quad (10)$$

The basis was adapted to the symmetry of the permutation-inversion group PI(C_{2v}), also called $C_{2v}(M)$.[48] The labeling of the irreducible representations (irreps) and the projection operators for this group are given in Table I.

III. COMPUTATIONAL DETAILS

All calculations were done on two different potential surfaces, the SQSBDE potential[25] by Quack and Suhm, and the more recent SO-3 potential[43] of Klopper, Quack, and Suhm. In the calculation of the expansion coefficients $c_{L_A L_B L}$ on the radial grid points, the integration over the angular coordinates [Eq. (9)] was performed by means of a Gauss–Legendre quadrature with 12 points for θ_X, and a Gauss–Chebyshev quadrature with also 12 points for ϕ. Since for certain grid points the potential becomes strongly repulsive, one would need extremely high terms in the expansion. To avoid this, the potential was damped in these repulsive regions by means of a tanh function up to a value $V_{\max}$:

$$\tilde{V} = \begin{cases} V, & V \leqslant V_0 \\ V_0 + \beta^{-1} \tanh[\beta(V-V_0)], & V > V_0, \end{cases} \quad (11)$$

where $\beta \equiv [V_{\max}-V_0]^{-1}$. With this scheme, the damped potential $\tilde{V}$ is continuous around V_0 up to the second derivative. Care was taken to use sufficiently high values of V_0 and $V_{\max}$, so that the potential was affected only in regions without physical meaning. The actual values used were $V_0 = 140\,000\ \mathrm{cm}^{-1}$, and $V_{\max}=2V_0$. The expansion of the potential was taken up to $L_A, L_B \leqslant 11$.

The dimer stretch basis functions were computed using a sinc function DVR on a reference potential, which was obtained by minimization of the potential in the monomer stretch coordinates, while keeping the intermolecular distance fixed at the grid points and the angles at their equilibrium values in the dimer. An equally spaced grid of 42 points in the range $4\,a_0 \leqslant R \leqslant 8\,a_0$ was used for both potentials.

The monomer stretch basis functions were obtained in a similar way, but two different reference potentials were used. The first one was the pure monomer potential $V^{(\mathrm{mon})}$, obtained by making a cut through the PES at very large R. The second was a dimer adapted potential $V^{(\mathrm{dim})} = [V_A^{(\mathrm{dim})} + V_B^{(\mathrm{dim})}]/2$, where $V_A^{(\mathrm{dim})}$ was obtained by minimizing the potential by varying R, r_B, θ_A, θ_B, and ϕ, while keeping r_A fixed on the grid points. Analogously, $V_B^{(\mathrm{dim})}$ was obtained by minimization in all coordinates but r_B. The average of the two monomer potentials was taken in order to preserve the exchange symmetry in the dimer. For the SQSBDE potential a grid of 20 equally spaced point between 1.0 and 2.9 a_0 was applied, whereas for the SO-3 potential a grid of 22 points between 1.0 and 3.1 a_0 was used.

Convergence was reached with an angular basis set with j_A and j_B up to $j_A^{\max}=13$, a dimer stretch basis up to $n^{\max}=6$, and a monomer stretch basis with $v_A+v_B \leqslant 2$, which lead to a maximum basis size of approximately 22 000 functions for the $K=0$ states, and 38 000 for $K=1$. For the monomer ground states, the lowest eigenstates were calculated with a direct variant of the Davidson algorithm.[5,49] This procedure was not feasible for the monomer stretch excited states, however, since these states lie in the middle of the spectrum of the Hamiltonian in this basis. Therefore, we used a three-step procedure in each symmetry block, where in the first step the Hamiltonian was calculated in a basis with only the $v_A+v_B \leqslant 1$ monomer stretch functions, leading to a matrix with a dimension of half the total number of primitive basis functions (i.e., $\approx$11000). Eigenstates of this matrix were calculated in an energy range of approximately 3800–4500 cm^{-1} above the ground state using the NAG routine F02FCF, which yielded approximately 500 eigenfunctions. These eigenfunctions were used as a new basis for the Hamiltonian, together with additional primitive basis functions with $|v_A v_B\rangle = |02\rangle$ and $|20\rangle$, resulting in a basis of approximately 7600 functions. The eigenstates in this basis were calculated in the same energy range. Finally, the resulting eigenfunctions were again combined with the $|11\rangle$ func-

TABLE II. Eigenvalues of the monomer stretch ground state ($v_1=v_2=0$) of $(HF)_2$ for total angular momentum $J=0$ and A_1 and B_1 symmetry, using the dimer adapted monomer stretch basis. Values are given in cm^{-1}, relative to the ground state of -1057.88 cm^{-1} for the SQSBDE potential and -1061.73 cm^{-1} for SO-3. $\langle R\rangle$, ΔR (both in a_0) and B (in cm^{-1}) are computed from the SO-3 wave functions.

Γ	n	$\nu_3\nu_4\nu_5\nu_6$	SQSBDE	SO-3	$\langle R\rangle$	ΔR	B
A_1	1	0000	0.00	0.00	5.24	0.21	0.2205
	2	0100	126.40	126.57	5.30	0.32	0.2166
	3	0020	160.62	162.93	5.30	0.28	0.2157
	4	0200	244.58	248.21	5.36	0.42	0.2132
	5	0120	275.03	273.03	5.33	0.37	0.2147
	6	0040	292.74	306.12	5.41	0.38	0.2086
	7	0300	355.37	367.55	5.51	0.53	0.2041
	8	0220	385.03	392.08	5.43	0.49	0.2089
	9	0140	400.05	425.17	5.49	0.49	0.2045
	10	0060	463.61	446.54	5.37	0.34	0.2114
	12	1000	425.36	483.48	5.34	0.28	0.2126
B_1	1	0011	380.56	423.05	5.29	0.22	0.2159
	2	0111	493.97	546.33	5.43	0.38	0.2071
	3	0031	574.80	605.04	5.30	0.24	0.2152
	4	0211	598.93	658.98	5.59	0.51	0.1975
	5	0131	679.82	723.97	5.46	0.42	0.2055
	6	0311	696.33	760.94	5.76	0.61	0.1877
	7	0051	784.59	814.21	5.34	0.31	0.2130
	8	0231	773.79	832.27	5.61	0.55	0.1968
	9	0411	790.51	857.20	5.81	0.66	0.1862
	10	1011	846.26	911.07	5.44	0.31	0.2053

tions (yielding $\approx$5500 functions), and the Hamiltonian matrix was diagonalized once more in the same energy range.

IV. RESULTS AND DISCUSSION

The first ten energy levels of the HF dimer with both monomers in their vibrational ground state are given for all four symmetry blocks in Tables II and III for total angular momentum $J=0$, and Table IV for $J=K=1$. For $J=0$, the antigeared bend (ν_3) fundamental and its tunneling partner have also been added. The tables show the energy levels for both the SQSBDE and the SO-3 potentials calculated in the dimer adapted monomer stretch basis. Also the expectation value and root mean square amplitude of the intermolecular distance R are given, as well as the rotational constant $B=\langle 1/2\mu R^2\rangle$. These three values were calculated from the SO-3 wave functions. For the $J=1$, $K=0$ states too, energies and wave functions were calculated. We found that the difference between the resulting eigenvalues and the $J=0$

TABLE III. As in Table II, for A_2 and B_2 symmetry.

Γ	n	$\nu_3\nu_4\nu_5\nu_6$	SQSBDE	SO-3	$\langle R\rangle$	ΔR	B
A_2	1	0001	378.82	420.83	5.29	0.22	0.2160
	2	0101	491.29	542.84	5.42	0.38	0.2080
	3	0021	544.68	571.46	5.31	0.25	0.2148
	4	0201	594.54	654.75	5.58	0.51	0.1982
	5	0121	641.54	685.21	5.45	0.42	0.2059
	6	0041	690.08	716.06	5.31	0.24	0.2145
	7	0301	688.74	755.34	5.77	0.62	0.1875
	8	0221	732.00	788.15	5.63	0.54	0.1955
	9	0141	788.56	831.27	5.46	0.42	0.2055
	10	0401	779.17	848.83	5.83	0.69	0.1850
B_2	1	0010	0.44	0.59	5.24	0.21	0.2204
	2	0110	127.37	129.69	5.32	0.33	0.2153
	3	0030	168.08	170.12	5.30	0.27	0.2160
	4	0210	246.23	254.51	5.43	0.45	0.2084
	5	0130	289.14	299.55	5.40	0.41	0.2097
	6	0050	339.22	341.49	5.30	0.27	0.2155
	7	0310	357.49	373.04	5.58	0.55	0.1997
	8	0230	402.60	421.29	5.54	0.53	0.2016
	9	0150	455.61	468.55	5.42	0.41	0.2081
	10	0410	463.59	482.02	5.60	0.57	0.1979
	11	1010	440.36	486.13	5.49	0.49	0.2039

TABLE IV. As in Tables II and III, for $J=K=1$.

Γ	n	$\nu_3\nu_4\nu_5\nu_6$	SQSBDE	SO-3	$\langle R\rangle$	ΔR	B
A_1,B_1	1	0000	39.60	38.68	5.22	0.20	0.2221
	2	0100	168.59	175.47	5.30	0.34	0.2169
	3	0020	214.95	209.32	5.25	0.25	0.2200
	4	0200	289.41	305.06	5.41	0.46	0.2100
	5	0120	328.52	330.97	5.28	0.35	0.2184
	6	0040	348.14	354.30	5.34	0.33	0.2134
	7	0001	366.67	398.66	5.33	0.22	0.2130
	8	0300	401.67	426.41	5.57	0.56	0.2003
	9	0220	436.28	453.96	5.42	0.49	0.2096
	10	0140	456.43	479.87	5.47	0.45	0.2056
A_2,B_2	1	0010	40.38	39.73	5.22	0.20	0.2220
	2	0110	169.90	178.64	5.32	0.35	0.2154
	3	0030	232.42	228.12	5.24	0.23	0.2202
	4	0210	291.24	309.22	5.45	0.46	0.2075
	5	0130	351.91	362.44	5.37	0.39	0.2124
	6	0011	361.26	397.15	5.33	0.23	0.2131
	7	0050	430.34	428.31	5.32	0.35	0.2156
	8	0310	404.20	431.13	5.53	0.54	0.2022
	9	0230	463.12	486.43	5.50	0.51	0.2039
	10	0111	472.41	507.02	5.38	0.34	0.2102

energies was $2B$ to within 10^{-4} cm^{-1}, while the expectation values and amplitudes of R were virtually the same as for the $J=0$ states. Therefore, these results are not shown here.

The results in the monomer stretch basis from the free HF potential are not given, since we found that using the dimer adapted functions gives a systematic improvement of the energy. This effect is hardly noticeable on the SO-3 potential, where the difference does not exceed 10^{-3} cm^{-1}, but is much stronger on the SQSBDE potential where differences up to 0.4 cm^{-1} occur. That the free monomer stretch functions are less than optimal for the SQSBDE potential has been shown before for the ground state by Mladenović and Lewerenz.[50]

The states are labeled with the standard set of quantum numbers $(v_1v_2v_3v_4v_5v_6)$, which correspond to the "free-H" monomer stretch (ν_1), "bound-H" monomer stretch (ν_2), in-plane antigeared (or *cis*) bend (ν_3), dimer stretch (ν_4), in-plane geared (or *trans*) bend (ν_5), and dimer torsion (ν_6) modes. Since interchange tunneling involves the same coordinate as the geared bend vibration, the B states, which are odd with respect to interchange, contain an extra node in the ν_5 tunneling path. Therefore, the ground B state is labeled (000010), and all B states have odd v_5, whereas v_5 is even for the A states. It follows that the geared bending fundamental is labeled (000020).

Comparison of the SQSBDE results for $J=0$ with the 6D results of Zhang *et al.*[33] shows that the energy levels are generally similar. The difference of 0.55 cm^{-1} in the dissociation energy may be explained by the fact that Zhang *et al.* used a monomer stretch basis obtained from the free HF potential, combined with the fact that they did not include the $v_A+v_B=2$ functions. Indeed, we found a dissociation-

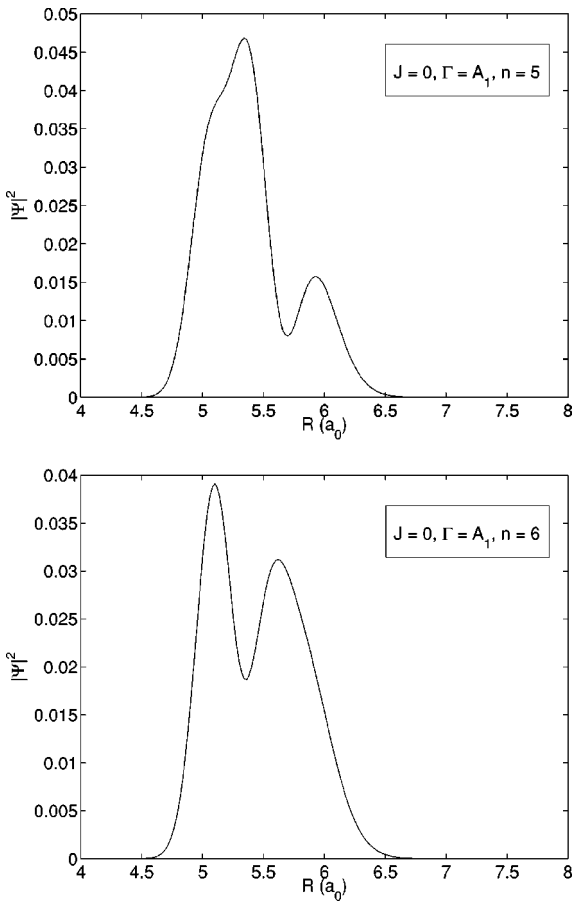

FIG. 2. Square modulus of the wave function as a function of R, integrated over all other coordinates, calculated on the SO-3 potential. The upper panel is the (000120) state, the lower the (000040) state. Both are for total angular momentum $J=0$.

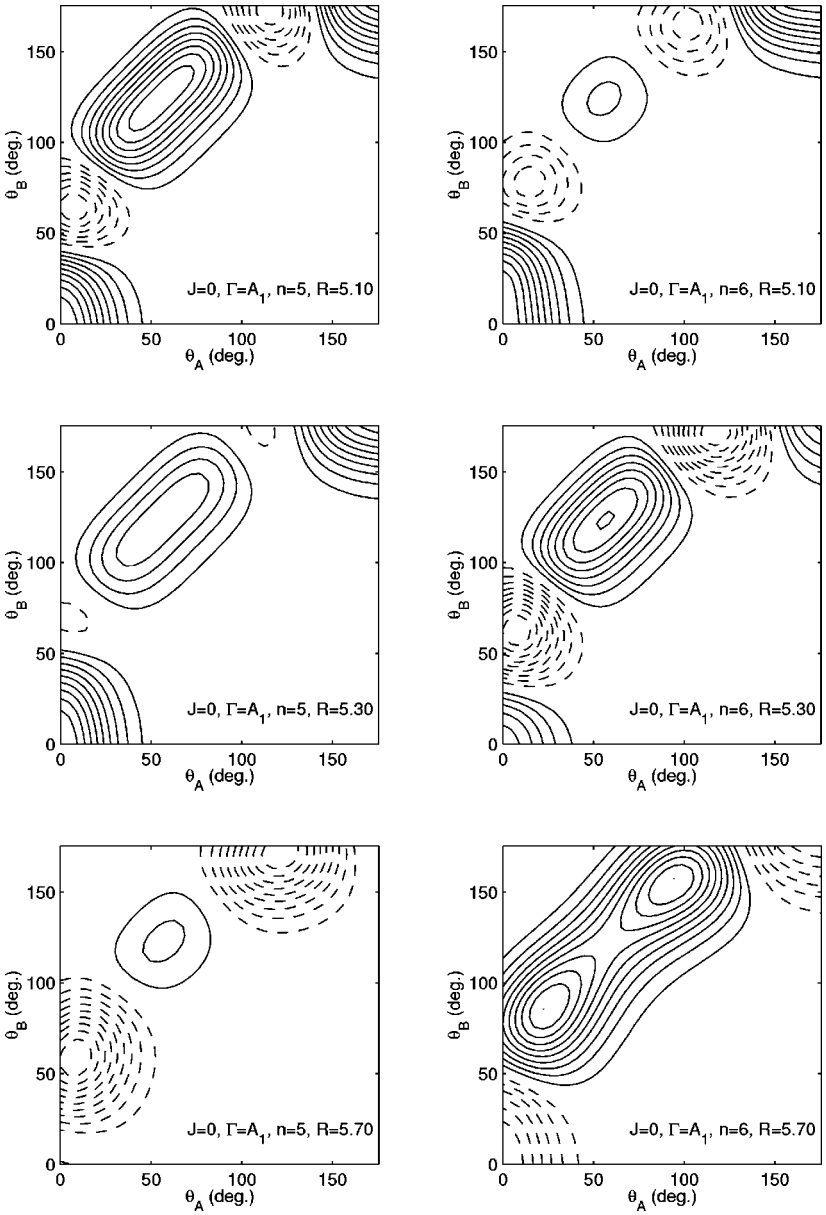

FIG. 3. Cuts through the wave function for the (000120) state (left), and the (000040) state (right) on the SO-3 potential for $J=0$. Both r_A and r_B are kept fixed at $1.769\,a_0$, and $\phi=180°$. The cuts are made for $R=5.1\ a_0$ (top), $5.3\ a_0$ (middle) and $5.7\ a_0$ (bottom).

energy of $1057.46\ \mathrm{cm}^{-1}$ when the free monomer basis was used, much closer to their value of $1057.33\ \mathrm{cm}^{-1}$.

The assignment of the quantum numbers to the states was done on the basis of nodal patterns in the wave functions, combined with energy considerations. For the SQSBDE bound states, the assignment of the v_4 stretch quantum number was facilitated by the strong correspondence between this quantum number and the expectation value and root mean square amplitude of R, an effect that is much less pronounced on the SO-3 potential. An example of the weaker correspondence of v_4 with $\langle R\rangle$ on the SO-3 potential can be seen in the fifth and sixth $J=0$ states of the A_1 irrep, where the higher stretch quantum number is assigned to the fifth state, despite the fact that the expectation value of R, as well as the amplitude, are smaller. A radial plot of the density (Fig. 2) does not give direct evidence for the given assignment either. Angular cuts through the wave function are not very helpful, since they change very much with R (see Fig. 3), so that this assignment can only be made on the basis of energy considerations. Similar situations occur for instance in the eighth and ninth states of the same A_1 irrep, as well as for their tunneling partners in the B_2 irrep.

An overview of the ground state energy splittings is given in Table V. Most of the splittings from the new SO-3 potential are in far better agreement with the available spectroscopic data than those obtained from the SQSBDE potential. The SO-3 dissociation energy of $1061.73\ \mathrm{cm}^{-1}$ is well within the error bars of the experimental number of $1062 \pm 1\ \mathrm{cm}^{-1}$, as obtained by Bohac *et al.*[21] This should not come as a surprise, since the SO-3 surface was refined to reproduce this number.[43] More interesting are the vibrational frequencies. Unfortunately, for the monomer stretch ground state modes in $(HF)_2$, the experimental data on the intermolecular frequencies are still scarce and rather uncertain, so that comparison between the two potentials is difficult. Looking at the data that are available, one can see that the performance of the PESs in this respect is rather alike, except for the ν_6 (dimer torsion) frequency. The most reliable com-

TABLE V. Comparison of calculated ground state energy splittings with experiment. Tunneling splittings between even (A) and odd (B) states with respect to monomer exchange are denoted by $\Delta(\nu)=E_\nu^- - E_\nu^+$.

	SQSBDE	SO-3	Expt.	Ref.
		$J=K=0$		
D_0	1057.88	1061.73	1062	21
$\Delta(\nu_0)$	0.44	0.59	0.658690	11
ν_3	425.36	483.48		
$\Delta(\nu_3)$	15.01	2.65		
ν_4	126.40	126.57	≈ 125	25
$\Delta(\nu_4)$	0.98	3.13	>2	25
$2\nu_5$	160.62	162.93	≈ 161	54
$\Delta(2\nu_5)$	7.47	7.19		
ν_6	378.82	420.83	≈ 419?	43
$\Delta(\nu_6)$	1.74	2.22		
		$J=K=1$		
ν_0	39.60	38.68	35.425	18
$\Delta(\nu_0)$	0.78	1.05	1.0643	12
ν_4	168.59	175.47		
$\Delta(\nu_4)$	1.30	3.17		
$2\nu_5$	214.95	209.32		
$\Delta(2\nu_5)$	17.47	18.80		
ν_6	366.67	398.66	399.79	55
$\Delta(\nu_6)$	5.41	1.51	1.63	55

parison in this mode is made for the $K=1$ state, since the experimental assignment of the ν_6 mode for $K=0$ is tentative.[43] Looking at this $K=1,\nu_6$ excitation, we see that the SO-3 result differs by only 0.3%, whereas the SQSBDE frequency is 8% off.

As another, more sensitive test we can compare the tunneling splittings between states of even (A_1 and A_2) and odd (B_2 and B_1) symmetry under monomer exchange. A tunneling pair is formed by a state of A_1 symmetry and the corresponding state of B_2 symmetry, or similarly between states of A_2 and B_1 symmetry. Note that the quantum numbers of the members of such a pair are equal, except for the ν_5 quantum, which is one higher for the B state. We see that the new potential reproduces with 0.59 cm^{-1} around 90% of the ground state tunneling splitting of 0.66 cm^{-1}.[11] Although this 6D number is somewhat less than the (4+2)D result of Klopper *et al.*,[43] who reported a tunneling splitting of 0.63 cm^{-1}, it is still a significant improvement over the SQSBDE potential, which only gives 67%. Also the tunneling splitting upon ν_4 excitation is consistent with the experimental lower limit, whereas the SQSBDE result is not. Again the most striking are the results for the tunneling splitting in the $K=1$, ν_6-excited state: whereas the SO-3 splitting is only 7% too low, the SQSBDE result is more than a factor of 3 too high.

Results for the monomer stretch excited states are given in Tables VI and VII. Several states in Tables VI and VII have been marked with an asterisk to indicate a relatively large mixing with vibrational ground state functions (>5%). Again the result for the free monomer basis is not shown, but since the choice of the monomer stretch basis has a greater effect for the excited states, the difference in results for the free monomer and dimer adapted basis sets are greater than in the ground state. The effect now also shows up for the SO-3 potential, with dimer adapted states that are up to 0.3 cm^{-1} lower than the corresponding free monomer states. It is still stronger on the SQSBDE potential, however, where differences up to 2 cm^{-1} occur.

The results for excited states of A_1 and B_2 symmetry on the SQSBDE surface may be compared with those of Wu *et al.*,[34] and those of Volobuev *et al.*[51] on the same surface. In general the results presented there are very similar to ours, with typical differences around 0.5 cm^{-1}.

For the stretch excited states, there are more experimental data available, thanks to the experiments of Pine and co-workers[16,18,19] and those of Anderson, Davis, and Nesbitt.[52,53] A comparison of our results with these data is given in Table VIII. We see again that the SO-3 potential

TABLE VI. As in Table II, for the first monomer stretch excited states ($v_1+v_2=1$).

Γ	n	$\nu_1\nu_2\nu_3\nu_4\nu_5\nu_6$	SQSBDE	SO-3	$\langle R\rangle$	ΔR	B
A_1	1	010000	3895.94	3867.09	5.21	0.22	0.2224
	2	100000	3939.94	3929.17*	5.26	0.29	0.2192
	3	010100	4034.47	4000.50	5.27	0.32	0.2185
	4	100100	4064.44	4043.22	5.28	0.27	0.2180
	5	010020	4065.57	4056.93	5.29	0.32	0.2177
	6	100020	4100.74	4096.22	5.29	0.28	0.2168
	7	010200	4161.10	4128.40*	5.43	0.49	0.2088
	8	100200	4181.74	4161.48	5.30	0.36	0.2174
	9	010120	4190.27	4182.62	5.39	0.43	0.2114
	10	010040	4206.48	4196.85	5.37	0.36	0.2116
B_1	1	010011	4283.72	4303.54	5.26	0.21	0.2184
	2	100011	4312.41	4353.21	5.29	0.24	0.2165
	3	010111	4405.38	4432.92	5.39	0.37	0.2104
	4	100111	4424.15	4475.15	5.35	0.35	0.2132
	5	010031	4464.58	4480.76	5.34	0.31	0.2133
	6	100031	4490.17	4514.13	5.29	0.24	0.2164
	7	010211	4515.92	4552.34	5.53	0.49	0.2015
	8	100211	4527.67	4590.37	5.53	0.49	0.2017
	9	010131	4566.05	4599.94	5.44	0.43	0.2071
	10	100131	4596.07	4629.26	5.31	0.28	0.2152

TABLE VII. As in Table III, for the first monomer stretch excited states ($v_1+v_2=1$).

Γ	n	$\nu_1\nu_2\nu_3\nu_4\nu_5\nu_6$	SQSBDE	SO-3	$\langle R\rangle$	ΔR	B
A_2	1	010001	4283.33	4303.00	5.27	0.23	0.2176
	2	100001	4312.91	4353.85	5.28	0.22	0.2172
	3	010101	4404.58	4431.93	5.38	0.37	0.2109
	4	100101	4425.12	4469.76	5.28	0.26	0.2171
	5	010021	4459.39	4479.06	5.40	0.37	0.2093
	6	100021	4496.68	4523.53	5.29	0.24	0.2163
	7	010201	4514.25	4551.14*	5.51	0.51	0.2037
	8	100201	4529.57	4588.57*	5.45	0.45	0.2073
	9	010121	4561.29	4594.26	5.53	0.48	0.2014
	10	100121	4600.35	4617.96	5.30	0.26	0.2158
B_2	1	010010	3896.04	3867.26	5.21	0.21	0.2225
	2	100010	3939.81	3929.01	5.22	0.21	0.2219
	3	010110	4034.88	4001.39*	5.31	0.36	0.2163
	4	100110	4063.67	4045.44	5.28	0.27	0.2179
	5	010030	4067.57	4055.56	5.28	0.32	0.2180
	6	100030	4098.48	4094.15	5.29	0.29	0.2166
	7	010210	4162.31	4130.62	5.37	0.42	0.2129
	8	100210	4180.19	4168.44	5.30	0.37	0.2174
	9	010130	4195.99	4181.23	5.38	0.42	0.2119
	10	010050	4208.28	4200.10	5.35	0.36	0.2130

performs better than SQSBDE. The calculated donor stretch frequency of 3867.09 cm^{-1} and the acceptor stretch at 3929.17 cm^{-1} calculated with the SO-3 potential are in much closer agreement with the experimental values of 3868.079 and 3930.903 cm^{-1} than their SQSBDE counterparts. Also the SO-3 dimer stretch ($\nu_{1,2}+\nu_4$) and geared bend ($\nu_{1,2}+\nu_5$) frequencies combined with excitation of either the donor or the acceptor stretch are very good. The errors between the results on this potential and experiment are 3.5–16 times smaller than the corresponding errors of the SQSBDE frequencies.

Also the tunneling splittings in these intramolecular stretch modes are better reproduced by the new potential. This effect can also be seen in the $\nu_1+\nu_4$ combination band, but is less pronounced in states in which the geared bend is excited (in fact, the tunneling splitting in the $\nu_1+2\nu_5$ states is even worse on SO-3, although not much). It would be interesting to measure the experimental tunneling splitting upon $\nu_2+\nu_4$ excitation, since the SO-3 splitting is more than twice as large as the SQSBDE result.

TABLE VIII. Comparison of calculated excited state energy splittings with experiment. Tunneling splittings between even (A) and odd (B) states with respect to monomer exchange are denoted by $\Delta(\nu)=E_\nu^- - E_\nu^+$.

	SQSBDE	SO-3	Expt.	Ref.
ν_1	3939.94	3929.17	3930.903	18
$\Delta(\nu_1)$	−0.12	−0.17	−0.215	18
ν_2	3895.94	3867.09	3868.079	18
$\Delta(\nu_2)$	0.09	0.18	0.233	18
$(\nu_1+\nu_4)-\nu_1$	124.50	127.76	129.237	52
$\Delta(\nu_1+\nu_4)$	−0.77	−1.38	−1.664	52
$(\nu_2+\nu_4)-\nu_2$	138.52	133.41	132.616	52
$\Delta(\nu_2+\nu_4)$	0.41	0.89		
$(\nu_1+2\nu_5)-\nu_1$	160.81	167.05	169.262	52
$\Delta(\nu_1+2\nu_5)$	−2.27	−2.07	−2.739	52
$(\nu_2+2\nu_5)-\nu_2$	169.63	176.13	178.667	52
$\Delta(\nu_2+2\nu_5)$	2.00	2.22	3.587	52
$(\nu_1+\nu_6)-\nu_1$	372.98	424.68		
$\Delta(\nu_1+\nu_6)$	−0.50	−0.64		
$(\nu_2+\nu_6)-\nu_2$	387.38	435.91		
$\Delta(\nu_2+\nu_6)$	0.39	0.54		

V. CONCLUSIONS

We have investigated the HF dimer by means of variational calculations of bound and quasibound states using the SQSBDE and SO-3 potential energy surfaces. Our results on the SQSBDE surface are comparable to previous studies. The choice of the monomer stretch basis is of considerable importance. Using a dimer adapted monomer stretch basis leads to significantly lower energies in most cases. In addition, we find that although the energy gap between $v_X=0$ and $v_X=2$ monomer stretch function is huge, these overtone functions have to be included in the basis for a good description of the bound and quasibound states.

To our knowledge, no calculations on $(HF)_2$ using the SO-3 potential have been published. We have made a side-by-side comparison of this potential with the older SQSBDE potential on the (quasi) bound states calculated. We find that many of the interesting features of the dimer can be computed with remarkable accuracy using the SO-3 potential. For the ground state, the dissociation energy is in perfect agreement with experiment. Also the intermolecular vibrational frequencies agree well with the available experimental data, especially in the case of ν_6 excitation, where the SQSBDE potential fails. Even the tunneling splittings, which are quite small, and very sensitive to the potential, are reproduced very well by the SO-3 potential, much better than by the older PES.

For the monomer stretch excited states, the difference between SO-3 and SQSBDE is even more striking. Not only are the ν_1 and ν_2 fundamental frequencies reproduced to within 2 cm^{-1} (as opposed to $\approx$30 cm^{-1} for SQSBDE), also the intermolecular frequencies built upon these intramolecu-

lar excitations all agree to within 1 or 2 cm^{-1}. The tunneling splittings in the excited states are not yet perfect, but are certainly an improvement over the SQSBDE tunneling splittings, which are typically too low by a factor of 2.

ACKNOWLEDGMENT

This research has been financially supported by the Council for Chemical Sciences of the Netherlands Organization for Scientific Research (CW-NWO).

[1] M. J. Elrod and R. J. Saykally, J. Chem. Phys. **103**, 921 (1995).
[2] Y. Qiu and Z. Bačić, J. Chem. Phys. **106**, 2158 (1997).
[3] Y. Qiu, J. Z. H. Zhang, and Z. Bačić, J. Chem. Phys. **108**, 4804 (1998).
[4] E. M. Mas, R. Bukowski, K. Szalewicz, G. C. Groenenboom, P. E. S. Wormer, and A. van der Avoird, J. Chem. Phys. **113**, 6687 (2000).
[5] G. C. Groenenboom, P. E. S. Wormer, A. van der Avoird, E. M. Mas, R. Bukowski, and K. Szalewicz, J. Chem. Phys. **113**, 6702 (2000).
[6] M. J. Smit, G. C. Groenenboom, P. E. S. Wormer, A. van der Avoird, R. Bukowski, and K. Szalewicz, J. Phys. Chem. A **105**, 6212 (2001).
[7] N. Goldman, R. Fellers, M. Brown, L. Braly, C. Keoshian, C. Leforestier, and R. Saykally, J. Chem. Phys. **116**, 10148 (2002).
[8] C. Leforestier, F. Gatti, R. Fellers, and R. Saykally, J. Chem. Phys. **117**, 8710 (2002).
[9] T. R. Dyke, B. J. Howard, and W. Klemperer, J. Chem. Phys. **56**, 2442 (1972).
[10] A. S. Pine and B. J. Howard, J. Chem. Phys. **84**, 590 (1986).
[11] W. J. Lafferty, R. D. Suenram, and F. J. Lovas, J. Mol. Spectrosc. **123**, 434 (1987).
[12] B. J. Howard, T. R. Dyke, and W. Klemperer, J. Chem. Phys. **81**, 5417 (1984).
[13] H. S. Gutowski, C. Chuang, J. D. Keen, T. D. Klots, and T. Emilsson, J. Chem. Phys. **83**, 2070 (1985).
[14] K. von Puttkamer and M. Quack, Chem. Phys. **139**, 31 (1989).
[15] J. M. Lisy, A. Tramer, M. F. Vernon, and Y. T. Lee, J. Chem. Phys. **75**, 4733 (1981).
[16] A. S. Pine and W. J. Lafferty, J. Chem. Phys. **78**, 2154 (1983).
[17] R. L. DeLeon and J. S. Muenter, J. Chem. Phys. **80**, 6092 (1984).
[18] A. S. Pine, W. J. Lafferty, and B. J. Howard, J. Chem. Phys. **81**, 2939 (1984).
[19] A. S. Pine and G. T. Fraser, J. Chem. Phys. **89**, 6636 (1988).
[20] Z. S. Huang, K. W. Jucks, and R. E. Miller, J. Chem. Phys. **85**, 3338 (1986).
[21] E. J. Bohac, M. D. Marshall, and R. E. Miller, J. Chem. Phys. **96**, 6681 (1992).
[22] M. D. Marshall, E. J. Bohac, and R. E. Miller, J. Chem. Phys. **97**, 3307 (1992).
[23] E. J. Bohac and R. E. Miller, J. Chem. Phys. **99**, 1537 (1993).
[24] D. C. Dayton, K. W. Jucks, and R. E. Miller, J. Chem. Phys. **90**, 2631 (1988).
[25] M. Quack and M. A. Suhm, J. Chem. Phys. **95**, 28 (1991).
[26] H. Sun and R. O. Watts, J. Chem. Phys. **92**, 603 (1990).
[27] M. Quack and M. A. Suhm, Chem. Phys. Lett. **234**, 71 (1995).
[28] M. D. Marshall, P. Jensen, and P. Bunker, Chem. Phys. Lett. **176**, 255 (1991).
[29] S. C. Althorpe, D. C. Clary, and P. R. Bunker, Chem. Phys. Lett. **187**, 345 (1991).
[30] D. H. Zhang and J. Z. H. Zhang, J. Chem. Phys. **98**, 5978 (1993).
[31] D. H. Zhang and J. Z. H. Zhang, J. Chem. Phys. **99**, 6624 (1993).
[32] W. C. Necoechea and D. G. Truhlar, Chem. Phys. Lett. **224**, 297 (1994).
[33] D. H. Zhang, Q. Wu, J. Z. H. Zhang, M. von Dirke, and Z. Bačić, J. Chem. Phys. **102**, 2315 (1995).
[34] Q. Wu, D. H. Zhang, and J. Z. H. Zhang, J. Chem. Phys. **103**, 2548 (1995).
[35] X. T. Wu, A. B. McCoy, and E. F. Hayes, J. Chem. Phys. **110**, 2354 (1999).
[36] X. T. Wu, E. F. Hayes, and A. B. McCoy, J. Chem. Phys. **110**, 2365 (1999).
[37] D. H. Zhang, Q. Wu, and J. Z. H. Zhang, J. Chem. Phys. **102**, 124 (1995).
[38] N. Halberstadt, P. Brechignac, J. A. Beswick, and M. Shapiro, J. Chem. Phys. **84**, 170 (1986).
[39] M. von Dirke, Z. Bačić, D. H. Zhang, Q. Wu, and J. Z. H. Zhang, J. Chem. Phys. **102**, 4382 (1995).
[40] M. E. Cournoyer and W. L. Jorgensen, Mol. Phys. **51**, 119 (1984).
[41] P. R. Bunker, P. Jensen, A. Karpfen, M. Kofranek, and H. Lischka, J. Chem. Phys. **92**, 7432 (1990).
[42] W. C. Necoechea and D. G. Truhlar, Chem. Phys. Lett. **248**, 182 (1996).
[43] W. Klopper, M. Quack, and M. A. Suhm, J. Chem. Phys. **108**, 10096 (1998).
[44] A. Sarsa, Z. Bačić, and J. W. Moskowitz, Phys. Rev. Lett. **88**, 123401 (2002).
[45] X.-G. Wang and T. Carrington, J. Chem. Phys. **115**, 9781 (2001).
[46] G. W. M. Vissers, G. C. Groenenboom, and A. van der Avoird, J. Chem. Phys. **119**, 286 (2003), following paper.
[47] G. C. Groenenboom and D. T. Colbert, J. Chem. Phys. **99**, 9681 (1993).
[48] P. R. Bunker and P. Jensen, *Molecular Symmetry and Spectroscopy*, 2nd ed. (NRC Research, Ottawa, 1998).
[49] E. R. Davidson, J. Comput. Phys. **17**, 87 (1975).
[50] M. Mladenović and M. Lewerenz, Chem. Phys. Lett. **321**, 135 (2000).
[51] Y. Volobuev, W. C. Necoechea, and D. G. Truhlar, J. Phys. Chem. A **101**, 3045 (1997).
[52] D. T. Anderson, S. Davis, and D. J. Nesbitt, J. Chem. Phys. **104**, 6225 (1996).
[53] D. T. Anderson, S. Davis, and D. J. Nesbitt, J. Chem. Phys. **105**, 4488 (1996).
[54] M. Quack and M. A. Suhm, Chem. Phys. Lett. **171**, 517 (1990).
[55] K. von Puttkamer and M. Quack, Mol. Phys. **62**, 1047 (1987).